

Dataset Obfuscation: Its Applications to and Impacts on Edge Machine Learning

Guangsheng Yu
Data61, CSIRO
Sydney, NSW, Australia
saber.yu@data61.csiro.au

Xu Wang
FEIT, UTS
Sydney, Australia
xu.wang-1@uts.edu.au

Ping Yu
Faculty of Computing, Harbin
Institute of Technology
Harbin, China
yuping0428@hit.edu.cn

Caijun Sun*
Zhejiang Lab
Hangzhou, China
sun.cj@zhejianglab.edu.cn

Wei Ni
Data61, CSIRO
Sydney, NSW, Australia
wei.ni@data61.csiro.au

Ren Ping Liu
FEIT, UTS
Sydney, Australia
renping.liu@uts.edu.au

ABSTRACT

Obfuscating a dataset by adding random noises to protect the privacy of sensitive samples in the training dataset is crucial to prevent data leakage to untrusted parties for edge applications. We conduct comprehensive experiments to investigate how the dataset obfuscation can affect the resultant model weights - in terms of the model accuracy, Frobenius-norm (F-norm)-based model distance, and level of data privacy - and discuss the potential applications with the proposed Privacy, Utility, and Distinguishability (PUD)-triangle diagram to visualize the requirement preferences. Our experiments are based on the popular MNIST and CIFAR-10 datasets under both independent and identically distributed (IID) and non-IID settings. Significant results include a trade-off between the model accuracy and privacy level and a trade-off between the model difference and privacy level. The results indicate broad application prospects for training outsourcing in edge computing and guarding against attacks in Federated Learning among edge devices.

CCS CONCEPTS

• **Computing methodologies** → **Machine learning; Artificial intelligence**; • **Security and privacy** → **Privacy-preserving protocols**;

KEYWORDS

data obfuscation, privacy, data leakage, machine learning, federated learning, edge computing

1 INTRODUCTION

Data privacy is one of the hotspots with various privacy-preserving solutions being proposed in terms of designing privacy-aware machine learning algorithms and platforms [1-4] or implementing cryptographic algorithms, such as homomorphic encryption, to encrypt the dataset [5] prior to a data disclosure. However, the privacy-aware machine learning algorithms address only the “hidden trees in a forest” problem by obfuscating the query results, and cannot prevent data leakage. On the other hand, homomorphic encryption is computationally intensive [6] and prohibitive for edge applications, and has to be carefully crafted in respect to different learning algorithms with weak generality [7].

Obfuscating a dataset using random noises recently came to the scene due to the increasing importance of data privacy in edge networks [8], particularly the training dataset privacy, in machine learning processes where edge-edge or edge-cloud dataset sharing is essential. A general practice of preserving data privacy is to add random noise to datasets during the data sharing to preserve the data privacy as one needs no compulsory presumptions about the trust between him/her and the data receivers. Existing studies evaluate only the impacts on model accuracy with no mention of either the model distance or the data utility which can outweigh the accuracy in many application scenarios [7]. The goal of this paper is to comprehensively investigate the impacts of noise-based dataset obfuscation on the trained models.

In this paper, we conduct comprehensive experiments regarding the dataset obfuscation in machine learning, to analyze in-depth the impacts on the resultant models and explore potential application scenarios in edge networks. The key contributions of this paper are as follows.

- (1) We determine a generic obfuscation model with various metrics considered over a training dataset.

*Caijun Sun acts as the corresponding author.

- (2) We carry out various types of experiments over the MNIST [9] and CIFAR-10 [10] datasets under both independent and identically distributed (IID) and non-IID conditions with a wide range of noise settings.
- (3) We discuss the challenges and potential applications in edge networks based upon the experimental results, including training outsourcing and Federated Learning (FL), with a new visualization tool, named Privacy, Utility, and Distinguishability (PUD)-triangle diagram.

The experiments show that the model accuracy declines with the increase of noise level. The increasing noise level also enlarges the model difference between feeding a raw dataset and its obfuscated version, thus weakening the training reproducibility. Also, the disguisability of fake datasets becomes stronger with the increase of noise level due to the subequal model differences. The resultant observation indicates the existence of a balanced stable point at which all metrics can be acceptable for real applications, including training outsourcing on edge computing and guarding against attacks in FL among edge devices.

The rest of the paper is organized as follows. Section 2 provides the background. The experiment settings and results are shown in Section 3, followed by discussions in Section 4. The related works are given in Section 5. Section 6 concludes the paper.

2 OVERVIEW OF DATASET OBFUSCATION

This section introduces important definitions in each step of the obfuscation model and key performance used to evaluate the impacts on the resultant models in the crafted experiments.

• Model Training

Given a dataset $T = \{t_i, l_i\}$ with t_i being the i -th sample in the dataset and l_i being the label of the sample, the model weights W can be trained with the training function \mathcal{F} .

$$W = \mathcal{F}(T). \quad (1)$$

The trained weights W can be tested on a testing dataset T_e and evaluated with the model prediction accuracy $\mathcal{A}(W)$.

• Data Obfuscation

We consider a uniform obfuscation of training data where IID noises are added to the training data, denoted by $T' = \mathcal{O}(T)$. The obfuscation function $\mathcal{O}(T)$ can be given by

$$\begin{aligned} t'_{ij} &= t_{ij} + \delta, \forall i \text{ and } j, \delta \sim \mathcal{N}(0, \sigma^2); \\ l'_i &= l_i; \end{aligned} \quad (2)$$

where t_{ij} is the j -th feature of t_i . R is the proportion of obfuscated data in the training dataset. Here we consider all training data is obfuscated by setting $R = 1$. $\delta \sim \mathcal{N}(0, \sigma^2)$

stands for the added Gaussian noise. The mean of the Gaussian noise is zero to ensure data utility.

• Model Difference

We use the Frobenius-norm (F-norm), i.e., $\|\cdot\|_F$, to measure the difference between two model weights, as given by

$$\mathcal{D}(W_i, W_j) = \|W_i - W_j\|_F = \sqrt{\sum_k |w_{ik} - w_{jk}|^2}. \quad (3)$$

w_{ik} and w_{jk} are the k -th entries of W_i and W_j , respectively.

3 EXPERIMENTS



(a) $\sigma = 0$ (b) $\sigma = 0.4$ (c) $\sigma = 0.8$ (d) $\sigma = 0$ (e) $\sigma = 0.4$ (f) $\sigma = 0.8$

Figure 1: Obfuscated MNIST (a, b, c) and CIFAR-10 (d, e, f).

In this section, we experimentally evaluate the impacts of adding random noise to training datasets on the resultant models. Experiments cover a range of Gaussian standard deviations and various IID and non-IID dataset settings.

3.1 Experiment Framework

3.1.1 System Settings. We train classification models using popular MNIST (10 labels and 60,000 training examples) and CIFAR-10 (10 labels and 50,000 training examples) datasets. Each of the datasets is randomly split into a global training dataset T_t with 90% data and a testing dataset T_e with the remaining 10% data. The classification model is a standard convolutional neural network (CNN) with six convolution layers and three max-pooling layers, named as \mathcal{M}_{cnn} . An initial model with random weights is used across all experiments. \mathcal{M}_{cnn} is trained with 180 epochs and the learning rate of 0.0001 on both datasets. The batch sizes for the training on MNIST and CIFAR-10 are 128 and 64, respectively.

We conduct the experiments upon the Ubuntu 20.04.3 with TensorFlow 2.7.0 GPU kernel in Python 3.7. The training runs on a local machine with the following specifications: 2x Intel(R) Xeon(R) Gold 6138 CPU @ 2.00GHz, 256GB RAM, 16TB of Disk Space, and 8x NVIDIA A100 40GB.

3.1.2 Training Dataset Settings. We generate the training datasets from the global T_t on IID and non-IID features respectively to show the impacts of training data on trained models. In the case of a non-IID dataset, we follow the non-IID data setting in [11] and consider Label-Skew-based and Quantity-Skew-based non-IID cases. We use “S- \mathcal{X} - \mathcal{Y} - \mathcal{Z} ” to represent the sampling settings of training datasets.

- Label degree \mathcal{X} : The dataset covers $\lfloor C\mathcal{X} \rfloor$ of the total C labels, where $C = 10$ for both datasets in this paper.
- Label overlapping ratio \mathcal{Y} : The dataset and its counterpart cover the same $\lfloor C\mathcal{X}\mathcal{Y} \rfloor$ labels.

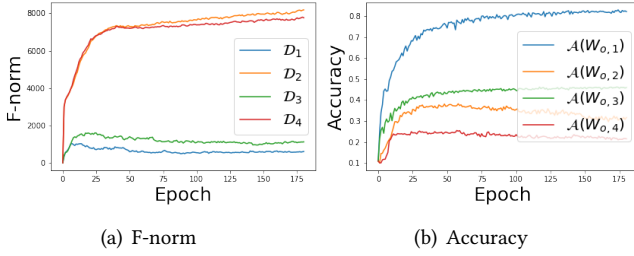


Figure 2: The dynamic F-norm and accuracy over epochs.

- Sampling ratio \mathcal{Z} : The dataset samples the entries of T_t with ratio \mathcal{Z} for each of the covered labels. The dataset contains $\mathcal{X}\mathcal{Z}|T_t|$ entries, where $|\cdot|$ gives cardinality.

3.2 Experiment Results and Evaluations

A first look at the data obfuscation over MNIST and CIFAR-10 by adding the random Gaussian noises is shown in Fig. 1.

We show the dynamics of model difference and model accuracy during training with CIFAR-10 in Fig. 2. A reference dataset T_r is sampled from T_t with setting S-1-1-0.5, i.e., covering all labels and containing half of the global data. T_r is also used as $T_{o,1}$, i.e., $T_{o,1} = T_r$, and obfuscated with $\sigma = 1$ for $T_{o,2}$, i.e., $T_{o,2} = \mathcal{O}(T_r)$, $\sigma = 1$. Dataset $T_{o,3}$ is sampled from T_t with setting S-0.5-1-1, i.e., covering half labels and containing all entries with the covered labels. $T_{o,4}$ is obfuscated $T_{o,3}$, i.e., $T_{o,4} = \mathcal{O}(T_{o,3})$, $\sigma = 1$. All datasets contain $0.5|T_t|$ entries. W_r and $W_{o,i}$ can then be obtained by training the initial model on T_r and $T_{o,i}$, respectively. $\mathcal{D}_i = \mathcal{D}(W_r, W_{o,i})$. Models are evaluated on T_e for accuracy $\mathcal{A}(W)$. Results in Fig. 2 show the convergence of both F-norm and accuracy over all (non-)IID and (non-)obfuscated settings. Note that the number of epochs used in all the experiments in this paper complies with that of Fig. 2.

We proceed to conduct four experiments over the MNIST and CIFAR-10 datasets from the following perspectives.

Exp-1 ($\mathcal{A}(W)$ vs. σ with different label degrees) - Figs. 3(a) and 3(b). The model weight $W_{1,1}$ is trained on the obfuscated dataset $\mathcal{O}(T_{1,1})$ that is sampled from T_t with setting S-1-1-0.5, and then evaluated on T_e for $\mathcal{A}(W_{1,1})$. $\mathcal{A}(W_{1,2})$ and $\mathcal{A}(W_{1,3})$ are obtained in the same way with settings S-0.8-1-0.625 and S-0.5-1-1, respectively. All the datasets contain $0.5|T_t|$ entries.

Exp-2 ($\mathcal{A}(W)$ vs. σ with different dataset sizes) - Figs. 3(c) and 3(d). The model weight $W_{2,1}$ is trained on the obfuscated dataset $\mathcal{O}(T_{2,1})$ that is sampled from T_t with setting S-0.8-1-1, and then evaluated on T_e for $\mathcal{A}(W_{2,1})$. $\mathcal{A}(W_{2,2})$ and $\mathcal{A}(W_{2,3})$ are obtained in the same way with settings S-0.8-1-0.5 and S-0.8-1-0.1, respectively. $T_{2,1}$, $T_{2,2}$ and $T_{2,3}$ cover the same eight labels and contain $0.8|T_t|$, $0.4|T_t|$, and $0.08|T_t|$ entries, respectively.

Exp-3 ($\mathcal{D}(W_r, W_o)$ vs. σ with different label overlapping ratios) - Figs. 4(a) and 4(b). $\mathcal{D}_{3,1} = \mathcal{D}(W_{r,3,1}, W_{o,3,1})$, where $W_{r,3,1}$ is trained from dataset $T_{r,3,1}$ that is sampled from T_t with setting S-0.5-1-0.5 and covers labels 0, 1, 2, 3 and 4. The reference dataset is also used as the obfuscated dataset for $W_{o,3,1}$, i.e., $T_{o,3,1} = T_{r,3,1}$, and the other reference datasets in this experiment, i.e., $T_{r,3,3} = T_{r,3,2} = T_{r,3,1}$. In terms of $\mathcal{D}_{3,2}$, $T_{o,3,2}$ is sampled from T_t with setting S-0.5-0.5-0.5 and covers labels 3, 4, 5, 6 and 7. For $\mathcal{D}_{3,3}$, $T_{o,3,3}$ is sampled from T_t with setting S-0.5-0.1-0.5 and covers labels 4, 5, 6, 7 and 8. All datasets contain $0.25|T_t|$ entries.

Exp-4 ($\mathcal{D}(W_r, W_o)$ vs. σ with different dataset sizes) - Figs. 4(c) and 4(d). $\mathcal{D}_{4,1} = \mathcal{D}(W_{r,4,1}, W_{o,4,1})$, where $W_{r,4,1}$ is trained on the dataset $T_{r,4,1}$ that is sampled from T_t with setting S-1-1-0.5 and contains $0.5|T_t|$ entries. The reference dataset is also used as the obfuscated dataset for $W_{o,4,1}$, i.e., $T_{o,4,1} = T_{r,4,1}$, and the other reference datasets in this experiment, i.e., $T_{r,4,3} = T_{r,4,2} = T_{r,4,1}$. In terms of $\mathcal{D}_{4,2}$, $T_{o,4,2}$ is sampled from T_t with setting S-1-1-0.25 and contains $0.25|T_t|$ entries. For $\mathcal{D}_{4,3}$, $T_{o,4,3}$ is sampled from T_t with setting S-1-0.1-0.05 and contains $0.05|T_t|$ entries.

Fig. 3 shows the decrease of the model accuracy with the increase of the noise level. The less diversified labels a training dataset contains, the lower accuracy the model can achieve over a fully-labeled testing dataset ($\mathcal{X} = 1$), as shown in Figs. 3(a) and 3(b). On the other hand, the models containing more data samples across covered labels can be more resistant to the adverse effect of obfuscation on the model accuracy, as shown in Figs. 3(c) and 3(d). This indicates that the accumulation of knowledge from the obfuscated samples is useful for recognizing the correct patterns.

It can be found in Fig. 4 that the F-norm $\mathcal{D}(W_r, W_o)$ increases with the noise level. This reflects that the obfuscated samples lead the model into a different direction of gradient descent, thus weakening the training reproducibility.

In Figs. 4(a) and 4(b), the gaps between the reference points, $\mathcal{D}_{3,1}$, and $\mathcal{D}_{3,2}$, and $\mathcal{D}_{3,3}$ at each given noise level are considered. The experiments on both MNIST and CIFAR-10 show that the gaps narrow down as the noise level increases. Given the same noise level, $\mathcal{D}_{3,3}$ tends to be more discriminable from $\mathcal{D}_{3,1}$ than $\mathcal{D}_{3,2}$ due to the lower label overlapping ratios \mathcal{Y} between $\mathcal{D}_{3,1}$ and $\mathcal{D}_{3,3}$. Also, having such a lower \mathcal{Y} can be more resistant to the impacts of obfuscation on the model difference, given that \mathcal{X} s are identical.

Figs. 4(c) and 4(d) are learned in concert with Figs. 3(c) and 3(d) in terms of the sampling ratio \mathcal{Z} . Given a certain number of epochs and identical \mathcal{X} s and \mathcal{Y} s, a smaller \mathcal{Z} leads to a smaller F-norm at a high level of obfuscation. This is because \mathcal{Z} corresponds to the size of dataset and is proportional to the number of learning steps per epoch with

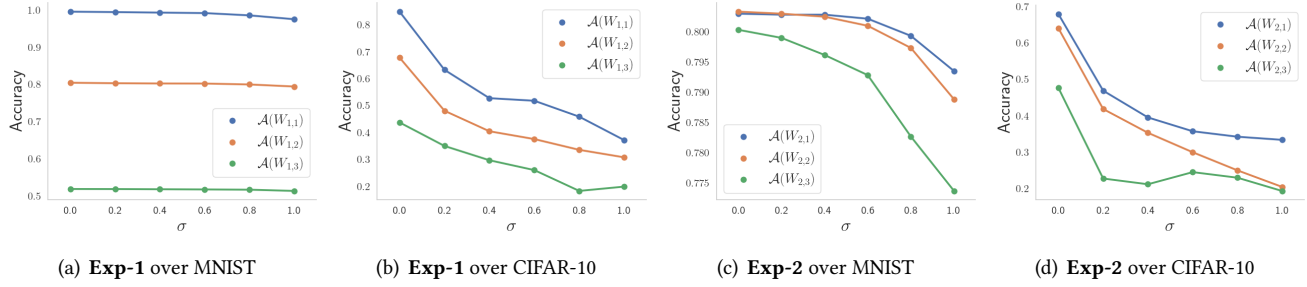


Figure 3: Model prediction accuracy over the testing dataset T_e along with the increase of noise level σ under different label degrees \mathcal{X} and sampling ratios \mathcal{Z} in MNIST and CIFAR-10 datasets, respectively. The x -axis is σ , and the y -axis gives the accuracy.

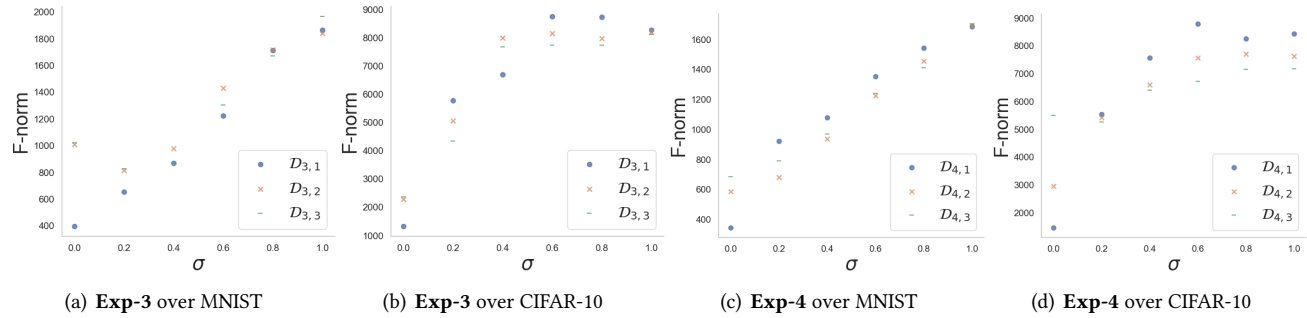


Figure 4: F-norm-based model difference between models trained from reference datasets without noise and obfuscated datasets along with the increase of noise level σ . The x -axis is σ for Gaussian noise, and the y -axis gives the F-norm values.

identical batch sizes, thus reducing the impacts of obfuscation and making $W_{o,4,2}$ and $W_{o,4,3}$ even closer to $W_{o,4,1}$ than $W_{r,4,1}$ is with $T_{o,4,1}=T_{r,4,1}$.

4 DISCUSSIONS

We discuss challenges of implementing dataset obfuscation, and explore real-world applications particularly on edge networks in this section. We first highlight the following three definitions,

- **Privacy**: the degree to which a training dataset T_{tr} is confused with T'_{tr} to prevent data leakage;
- **Utility**: the degree to which the obfuscated dataset T'_{tr} can be utilized to allow the local model to achieve acceptable model prediction accuracy upon the testing dataset;
- **Distinguishability**: the degree to which the F-norm gap Δ associated with a raw training dataset T_{tr}^i between its obfuscated dataset T'_{tr}^i and a different dataset T_{tr}^j with the same level of obfuscation.

$$\Delta = |\mathcal{D}(W_{T_{tr}^i}, W_{T'_{tr}^i}) - \mathcal{D}(W_{T_{tr}^i}, W_{T_{tr}^j})|, \text{ where } i \neq j. \quad (4)$$

The PUD-triangle refers to the levels in terms of the degree and nature of **Privacy**, **Utility**, and **Distinguishability**, as

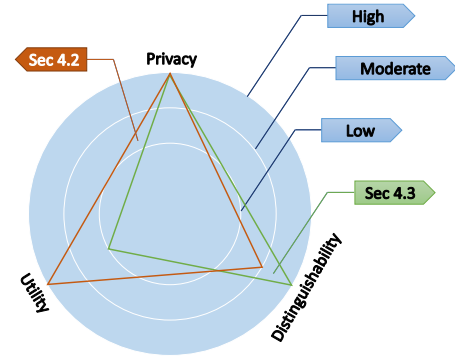


Figure 5: Two examples of the PUD-triangles.

illustrated in Fig. 5. We discuss in the following that different applications - examples are given in Sections 4.2 and 4.3 - satisfy different balance points among the PUD.

4.1 Privacy Decline

The more times an obfuscated training dataset T'_{tr} is disclosed, the more likely the raw dataset T_{tr} is exposed by simply calculating the average, if the noises are mutually IID among each sharing. One possible solution could be training

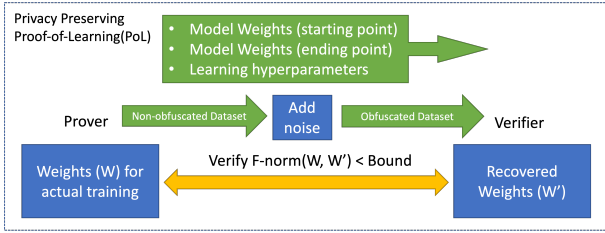


Figure 6: The workflow of Privacy-Preserving PoL.

over multiple finer-grained subsets which are further sampled from the entire local training dataset T_{tr} , and applying the non-IID noise along the training process.

4.2 Training outsourcing on Edge Networks

Model memorization attacks [12] can be exploited in a corrupted training outsourcing task on edge networks. Edge devices with relatively constrained capabilities would have to outsource the training task to the clouds or upper edges by sharing the training dataset. A malicious cloud-based service provider, as the outsourcee, may disclose the raw training dataset T_{tr} to its conspirators by encoding them into the model parameters. Thus, improving the **Privacy** by the dataset owners (i.e., training outsourcers) obfuscating the dataset before outsourcing them into the machine learning services, as suggested in [7]. Our experiment results reveal that the model prediction accuracy upon the testing dataset T_e is considered acceptable at over 80% on simple tasks with all samples being obfuscated; see Figs. 3(a) and 3(b).

4.3 Proof-of-Learning in FL

The PUD-triangle is particularly useful in a scenario where the model ownership and the proof of “works” for training are both crucial, e.g., the defenses against the model stealing attacks in FL [13]. Stealing others’ models and faking the ownership can be misleading to those who wish to ensure the necessary training overhead. By launching this attack, a malicious edge device with relatively powerful capability can cheat the whole edge network in regards to the amount of “works” that it has done, and steal the rewards. Proof-of-Learning (PoL) was proposed as a defense strategy against the model stealing attack [13], which requires the verifiers to replay part of the gradient descent and compare the resultant weights in terms of F-norm \mathcal{D} based on the training dataset T_{tr} shared by the prover (i.e., the owner of the dataset); see details in Fig. 6.

Edge devices implementing PoL in FL tasks have to share the training dataset T_{tr} , which is contrary to the original design intent of FL to preserve the privacy of T_{tr} . Adding random noises to obfuscate T_{tr} helps preserve privacy. However, this concept comes across two possible issues:

- Excessive noise added to T_{tr}^i causes a hard differentiation between its obfuscated version $T_{tr}^{i'}$ and an arbitrary obfuscated dataset $T_{tr}^{j'}$. This is known as the strong disguisability of fakes. By sharing a different dataset, a malicious “prover” can invalidate the PoL.
- Too good utility for an obfuscated dataset T_{tr}^i can anyhow enrich verifiers’ local datasets. Those who abuse the PoL by raising PoL challenges against as many models as possible can easily outperform those who are challenged due to the unbalanced size of the local training dataset under a non-IID setting.

We propose to settle at a balanced stable point where spoofing the dataset and abusing the PoL to enrich local resources can be prevented, i.e., maximizing **Distinguishability** and minimizing the **Utility**, while featuring a high level of **Privacy**. Figs. 4(a) and 4(b) show the feasibility of meeting the above requirement; see Section 3.2.

5 RELATED WORK

Protecting privacy in machine learning has attracted wide attention and spawned many approaches in terms of collaborative learning where datasets are locally used at edge devices with only small subsets of parameters shared [2], obfuscating the local model parameters by using random noise or differential privacy at edge devices [14], adopting homomorphic encryption to encrypt data samples [3], etc.

This paper focuses on protecting dataset privacy in tasks where sharing datasets is essential between edges or between edge and cloud. Authors of [7] focus on the training outsourcing and propose an OBFUSCATE function to obfuscate training datasets before the disclosure. The function adds random noises to data samples or augments datasets with new samples to protect the dataset privacy. The authors also show that training upon the obfuscated dataset can preserve the model accuracy. Our paper conducts more comprehensive experiments to investigate impacts on not only the model accuracy, but also the model difference under both IID and non-IID settings (the latter of which is yet to be considered in existing studies). We explore and discuss real-world applications in edge computing which can take advantage of dataset obfuscation by also establishing the PUD-triangle to visualize the requirement preferences.

6 CONCLUSION

We conducted comprehensive experiments to investigate how obfuscating a training dataset by adding random noises would affect the resultant model in terms of model prediction accuracy, model distance, data utility, data privacy, etc. Experimental results over both the MNIST and CIFAR-10 datasets revealed that, if a balanced point among all the considered metrics is satisfied, broad application prospects on

real-world applications will become realistic, including training outsourcing on edge computing and guarding against attacks in FL among edge devices.

REFERENCES

- [1] Martin Abadi, Andy Chu, Ian Goodfellow, H. Brendan McMahan, Ilya Mironov, Kunal Talwar, and Li Zhang. Deep learning with differential privacy. In *Proceedings of the 2016 ACM SIGSAC Conference on Computer and Communications Security, CCS '16*, page 308–318, New York, NY, USA, 2016. Association for Computing Machinery.
- [2] Reza Shokri and Vitaly Shmatikov. Privacy-preserving deep learning. In *Proceedings of the 22nd ACM SIGSAC Conference on Computer and Communications Security, CCS '15*, page 1310–1321, New York, NY, USA, 2015. Association for Computing Machinery.
- [3] Ehsan Hesamifard, Hassan Takabi, Mehdi Ghasemi, and Rebecca N Wright. Privacy-preserving machine learning as a service. *Proceedings on Privacy Enhancing Technologies*, 2018(3):123–142, 2018.
- [4] Olga Ohrimenko, Felix Schuster, Cedric Fournet, Aastha Mehta, Sebastian Nowozin, Kapil Vaswani, and Manuel Costa. Oblivious Multi-Party machine learning on trusted processors. In *25th USENIX Security Symposium (USENIX Security 16)*, pages 619–636, Austin, TX, August 2016. USENIX Association.
- [5] Raphael Bost, Raluca Ada Popa, Stephen Tu, and Shafi Goldwasser. Machine learning classification over encrypted data. *Cryptology ePrint Archive*, Paper 2014/331, 2014. <https://eprint.iacr.org/2014/331>.
- [6] Abbas Acar, Hidayet Aksu, A. Selcuk Uluagac, and Mauro Conti. A survey on homomorphic encryption schemes: Theory and implementation. *ACM Computing Surveys*, 51(4), jul 2018.
- [7] Tianwei Zhang, Zecheng He, and Ruby B. Lee. Privacy-preserving machine learning through data obfuscation. *CoRR*, abs/1807.01860, 2018.
- [8] Jiale Zhang, Bing Chen, Yanchao Zhao, Xiang Cheng, and Feng Hu. Data security and privacy-preserving in edge computing paradigm: Survey and open issues. *IEEE Access*, 6:18209–18237, 2018.
- [9] Y. Lecun, L. Bottou, Y. Bengio, and P. Haffner. Gradient-based learning applied to document recognition. *Proceedings of the IEEE*, 86(11):2278–2324, 1998.
- [10] Alex Krizhevsky et al. Learning multiple layers of features from tiny images. 2009.
- [11] Qinbin Li, Yiqun Diao, Quan Chen, and Bingsheng He. Federated learning on non-iid data silos: An experimental study. *arXiv preprint arXiv:2102.02079*, 2021.
- [12] Congzheng Song, Thomas Ristenpart, and Vitaly Shmatikov. Machine learning models that remember too much. In *Proceedings of the 2017 ACM SIGSAC Conference on Computer and Communications Security, CCS '17*, page 587–601, New York, NY, USA, 2017. Association for Computing Machinery.
- [13] Hengrui Jia, Mohammad Yaghini, Christopher A. Choquette-Choo, Natalie Dullerud, Anvith Thudi, Varun Chandrasekaran, and Nicolas Papernot. Proof-of-learning: Definitions and practice. In *2021 IEEE Symposium on Security and Privacy (SP)*, pages 1039–1056, 2021.
- [14] Yunlong Lu, Xiaohong Huang, Yueyue Dai, Sabita Maharjan, and Yan Zhang. Differentially private asynchronous federated learning for mobile edge computing in urban informatics. *IEEE Transactions on Industrial Informatics*, 16(3):2134–2143, 2020.